IOP Conf. Series: Materials Science and Engineering **249** (2017) 012020 doi:10.1088/1757-899X/249/1/012020

Aerodynamic characteristics and heat radiation performance of sportswear fabrics

H Koga[1], M Hiratsuka[2], S Ito[2] and A Konno[2]

[1],Graduate School of Kogakuin University, 1-24-2 Nishi-Shinjuku, Shinjuku-ku, Tokyo, 163-8677 Japan.
[2] Kogakuin University, 1-24-2 Nishi-shinjuku, Shinjuku-ku, Tokyo, 163-8677,Japan,;

ito@cc.kogakuin.ac.jp

Abstract. Sports such as swimming, speed skating, and marathon are sports competing for time. In recent years, reduction of the fluid drag of sportswear is required for these competitions in order to improve the record. In addition, sweating and discomfort due to body temperature rise during competition are thought to affect competitor performance, and heat radiation performance is also an important factor for sportswear. The authors have measured fluid force drag by wrapping cloth around a cylinder and have confirmed their differences due to the roughness of the fabric surface, differences in sewing. The authors could be verified the drag can be reduced by the position of the wear stitch. This time, we measured the heat radiation performance of 14 types of cloths whose aero dynamic properties are known using cylinders which are regarded as human fuselages, and found elements of cloth with heat radiation performance. It was found to be important for raising the heat radiation performance of sportswear that the fabric is thin and flat surface processing.

1. Introduction

With the advent of a new type of swim suit represented by a laser racer in recent years, the field of sportswear development attracts attention. Although the swim suit was banned, it proved that the time record was shortened by sportswear. It is important to pursue improvement of sportswear performance in time competing games. Due to its hydrodynamic performance, the swim suit mentioned above was also applied to various kinds of sporting events due to its functionality [1]. Improvement in the performance of sportswear that suits within the regulations is pursued in sports competing for recording not only for swimming events. Since sports motion involves a reciprocating action, Luth et al. [2] measures the hysteresis of fabric drag using a cylinder, and the rough material is said to have less drag reduction and less hysteresis. Chowdhury et al. [3][4] predicted the drag of the human body by measuring ski jumping and bicycle attitude aerodynamic position mainly and treating the human body as a combination of cylinders and measuring the drag of the inclined cylinder that is composed.

In order to find a sportswear with good aerodynamic characteristics and heat radiation performance, we measured the fluid force of several kinds of cloths using cylinder regard as a human torso, and also checked the drag at actual wearing using a mannequin did. The influence on arm torso was also measured by PIV. Furthermore, perspiration and discomfort due to body temperature rise during competition are thought to affect competitor performance, and heat radiation performance is also an important factor for sportswear, so we confirmed the heat radiation performance as well.

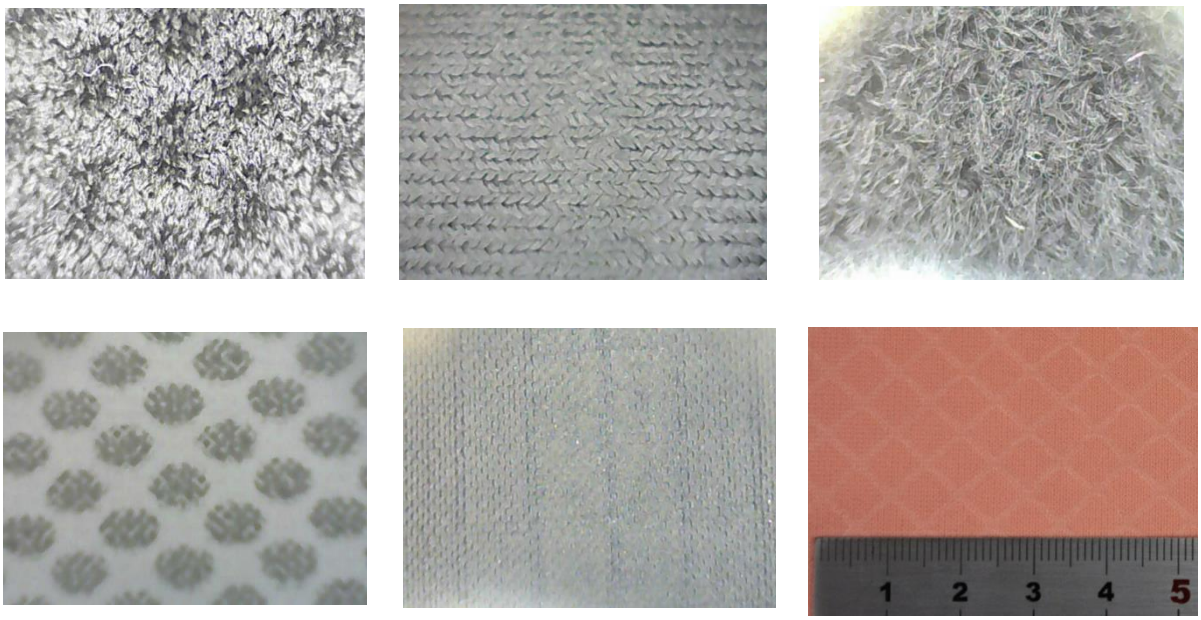

Figure 1. Examples of Fabrics investigated on aerodynamic properties

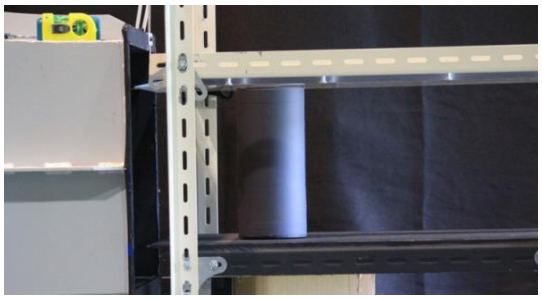

Figure 2. Pressure drag measurement system

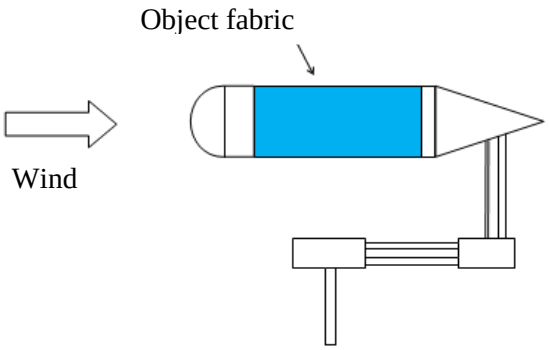

Figure 3. Friction drag measurement system

2. Experiment

A part of the sample cloth materials is shown in Figure 1. They were composed of different fabrics (woven fabric, knitted fabric), different surface roughness, fabrics with different surface finish.

2.1 Fluid-Force measurement

There are two types of drag: pressure drag by shape and friction drag by surface friction. Regarding the pressure drag which varies according to the flow pattern, a phenomenon called drag crisis in which the drag coefficient decreases abruptly as the Reynolds number, *Re*, increases in a uniform flow past a sphere or a cylinder is known. Achenbach [5], [6] conducted wind tunnel experiments on spherical balls, *Re* at which drag crisis occurs (Critical *Re* number) was about 3×10^5. In addition, it was found that the critical *Re* decreases by giving roughness to the sphere [5]. By using this mechanism, it is possible to grasp minute changes in fabrics as drag change. This pressure drag is proportional to the square of velocity. On the other hand, the friction drag is also related to the roughness of the surface and is proportional to the magnitude of the velocity. Using a low turbulence wind tunnel with a rectangular cross section of 380 mm × 380 mm, we changed the wind velocity from 6 to 30 m/s every 1 m/s in order to change the Reynolds number, and we measured the fluid drag of poly vinyl chloride, PVC, pipes with ϕ114mm, 240mm tall. Figure 2 shows the state of a vertical support type experimental apparatus for

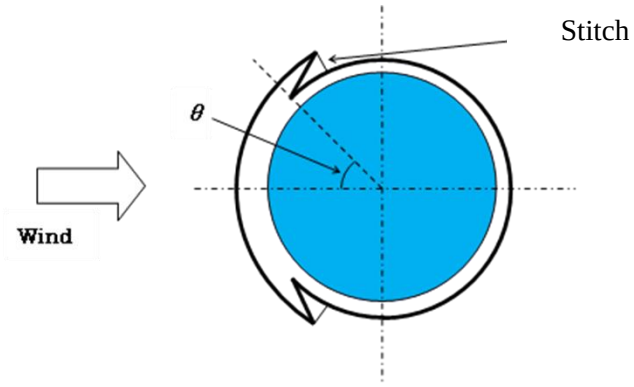

Figure 4. Outline of stitch position

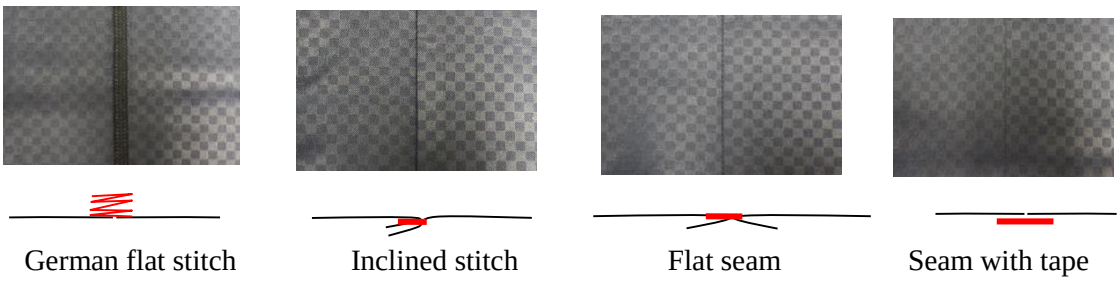

Figure 5. Seam/Stich of cloth

pressure drag, and Figure 3 shows a cobra type experimental apparatus for friction drag. In the friction drag measurement, the friction drag of the cloth was measured by removing the tare drag of the setting jig in order to measure the friction of only the cylinder to which the cloth was attached.

2.2 Stich position and its shape

In the pressure drag, the drag by different sewing positions in the same fabric wrapped around a cylinder as shown in Figure 4 was measured, and the drag which changed according to the difference of the stich shape as shown in Figure 5 was confirmed. Furthermore, the pressure drag of the cylinder with false stitch attached by a thick thread as shown in Figure 6 was also measured.

2.3 Mannequin Experiment

As shown in Figure 7, using a Goettingen type large wind tunnel facility with a size of 1800 mm × 1800 mm, 0.1% maximum wind speed of 56 m/s, the pressure drag of a full-size mannequin was measured, dressed in whole-body tights with false stitchs as 2, 5 thread of ϕ0.7mm thick flatly or stereoscopically, with masked tape at the curved side surface.

2.4 Experiments on cylinders with arms

Fluid force measurement and PIV measurement were carried out on a cylindrical model with arm on which cloth was attached, reflecting the result of using a human body model. By connecting two small cylinders of ϕ30 mm to PVC cylinder of ϕ114 mm shown in Figure 8, the cylinder with arms model simulates the body trunk with arm. The cloth was attached on them and the fabric having the lowest

Figure 6. A thread with adhesive tape simulating a stitch

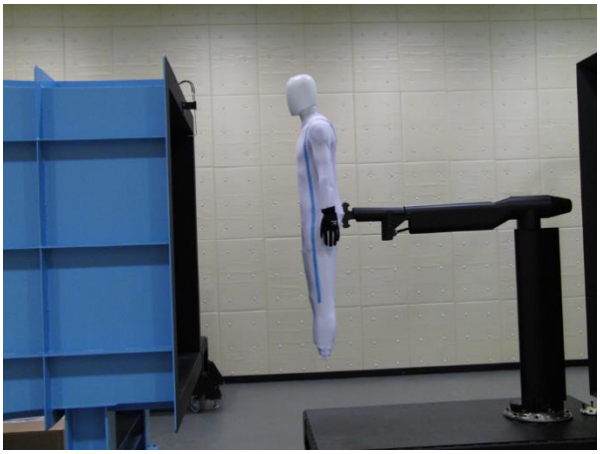

Figure 7. Full-size mannequin with false stitches at wind tunnel facility

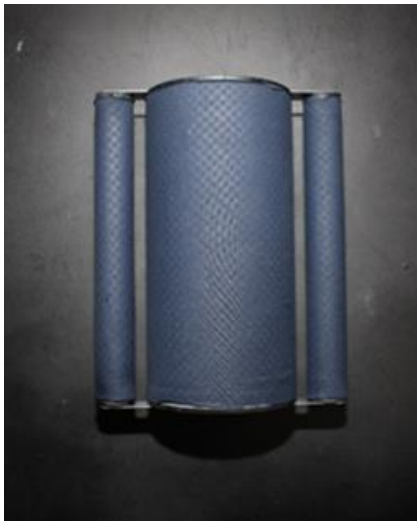

Figure 8. Test cylinder with arms

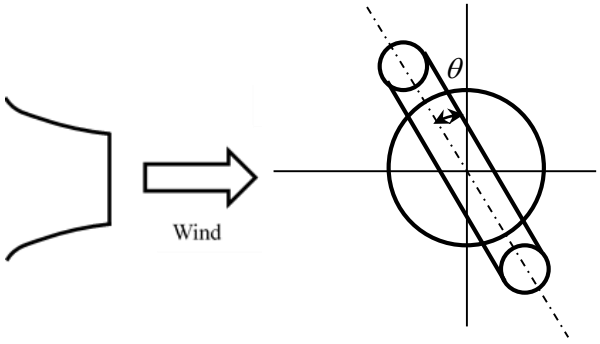

Figure 9. Definition of slant angle θ

drag was used, and the stitch position with the lowest pressure drag was made at an tilt angle θ of 60° as shown in Figure 9 with respect to the wind direction. PIV measurements were made at 10 m/s and 27 m/s before and after drug crisis based on the drag test results. In the PIV measurement, an average image obtained by translating the light source and the camera in order to cover the narrowness of the area was combined.

2.5 Heat radiation experiment

14 types of cloths were attached around the cylindrical model partly shown in Figure 1 and the ground plate was placed at the lower end. Heat radiation performance measurement was carried out using infrared thermography camera (R 500 EX) thermography of Nippon Avionics Co., Ltd. In the cylindrical model, a silicone rubber heater was wrapped around a vinyl chloride cylinder of ϕ 114 mm, and cloth was stuck thereon. The heat radiation performance test was conducted in a state where the room

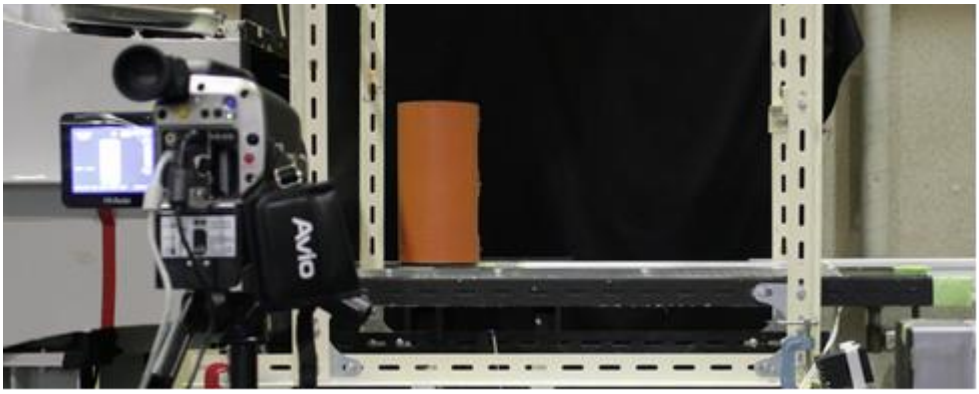

Figure 10. Thermal Experimental setup

temperature was controlled to 22 °C by air conditioning. By setting the voltage to 20.4 Volt using the direct current stabilized power supply, the average surface temperature of the heater was set to 40 °C, at first. A cover was placed on the test cylinder and the energization was cut off in order to keep its temperature. After driving the wind tunnel, when reaching the prescribed speed, i.e. 3, 6, 9, 12, 15 m/s, remove the cover and energize the heater. The ventilation time for each wind speed was shown in Table 1. And the surface temperature was photographed by thermography. Regarding the ventilation time, it was set the time when the heater without cloth became below 35 °C as shown in Table 1. The ventilation time was different for each wind speed.

Table 1. Wind velocity and ventilation time

Wind velocity [m/s]	3.0	6.0	9.0	12.0	15.0
Ventilation time [s]	90	75	60	45	30

3. Result and Discusion

The drag coefficient C_D, the friction drag coefficient C_f and the Reynolds number R_e are represented in Eqs. (1), (2) and (3). A: section area of the cylinder [m^2], d: diameter of the cylinder [m], ν: kinematic viscosity of air [m^2/s], D: drag force [N], D_f: drag force by friction[N], ρ: air density[kg/m^3], U: velocity of uniform flow[m/s].

$$C_D = \frac{D}{\frac{1}{2}\rho U^2 A} \tag{1}$$

$$C_f = \frac{D_f}{\frac{1}{2}\rho U^2 A} \tag{2}$$

$$Re = \frac{Ud}{\nu} \tag{3}$$

3.1 Fluid-Force measurement

3.1.1 Pressure drag coefficient C_D

Figure 11 shows some results of pressure drag. The drag crisis could not be seen on the base material of the PVC pipe which has a smooth surface shown in the curve of Tare. In some fabrics, drag crisis has

occurred from the area of $Re = 0.4 \times 10^5$,i.e. curve “a”, depending on the roughness of the fabric. As the *Re* number increases, that is, as the speed increases, the laminar boundary layer transitions to the turbulent boundary layer, and the separation point shifts backward along with the cylinder surface, and the drag reduction occurs in the region with low *Re* in this region. The value of C_D after the criticality gradually increased with the roughness of the surface was seen.

3.1.2 Friction drag coefficient C_f

The surface of PVC pipe which has smooth surface showed the lowest value in Figure12. Fabrics except Fabric "a" have to gradually rise as the speed rises. The "a" has a fabric with relatively high roughness, but due to the unique roughness shape C_f was going down as the velocity rose. The friction drag increases as transitioning from the laminar boundary layer to the turbulent boundary layer. The C_f of the fabric similar to the smooth surface is low, and the C_f of the texture transitioning to the coarse turbulent

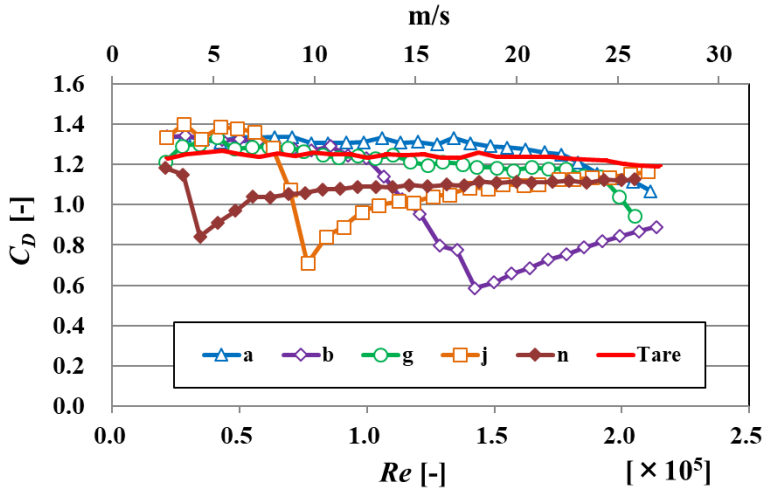

Figure 11. Pressure drag coefficient

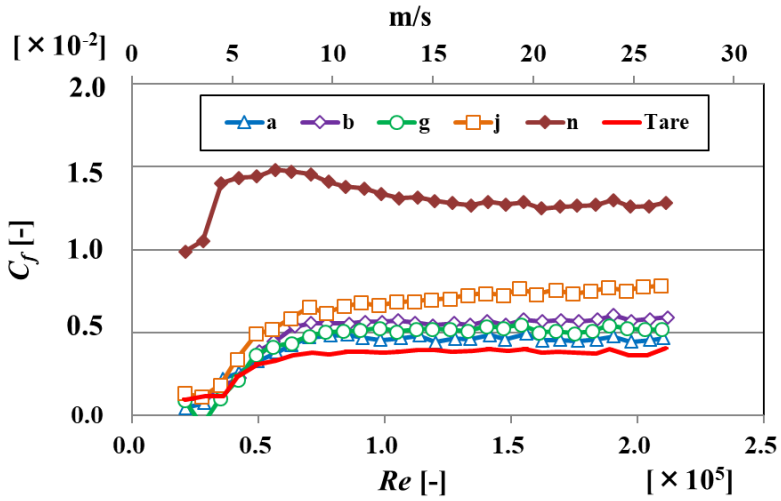

Figure 12. Skin friction drag coefficient

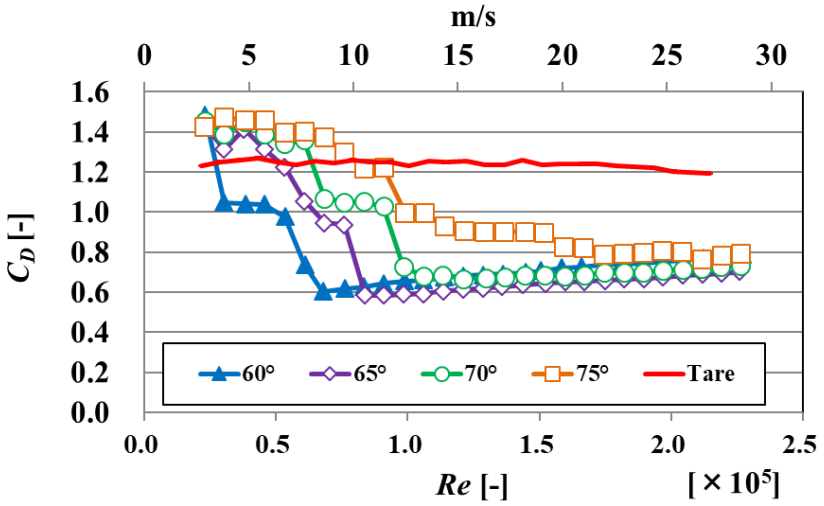

Figure 13. Differences of pressure drag by the positions of stiches

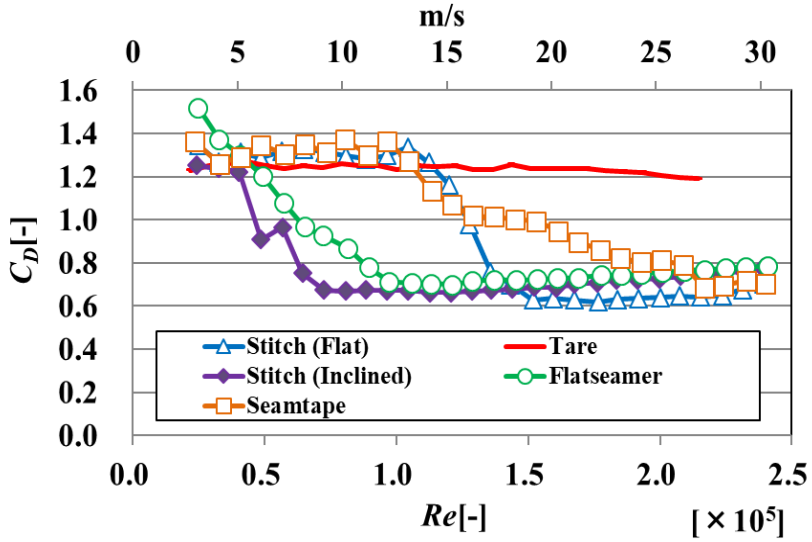

Figure 14. Differences of pressure drag among the different stitch types

boundary layer tends to be turbulent high. It was also found that the influence of *Re* number on friction drag was not large.

3.2 Stich position and its shape

3.2.1 Difference in stitch position

The pressure drag varies greatly due to the difference in turbulent transition position. Figure 13 shows the change in the pressure drag caused by the difference in the position of the cylinder symmetrical stitch using the same fabric. The data of the surface of PVC pipe is a line without mark indicated by Tare, but in this Reynolds number region it does not show drag crisis. However, due to the difference in positions of stitches, The "60°" reaches the supercritical region from the Reynolds number around 0.6×10^5, shows C_D = 0.6 and half the drag coefficient of the C_D = 1.2 of the smooth surface. The Reynolds number becomes high, it is understood that the values of C_D s of every position is maintained to the same extent.

3.2.2 Difference in stitch shape

As mentioned above, the pressure drag varies depending on the difference in the separation point, an attempt was made to forcibly generate a turbulent flow transition by changing the stitch shape as shown in Figure 5 and to reduce the drag. The stitch position is constant, and the drag force depending on the stitch shape is shown in Figure 14. It can be seen that drag crisis also occurs from around 0.6×10^5 shown in the figure and keeps the low drag as it is. It can be seen that there is a stitch shape that has the effect of fixing the separation point.

3.3 Mannequin Experiment

Figure 15 shows the C_D of the mannequin by the false stitch on the mannequin side surface by various combination of thick threads. The drag crisis seen at the stitch position of the cylinder did not appear in the mannequin and whole the C_D curves are shown as a nearly flat. The wake, related to the pressure drag, started from the flow separation point of the body trunk by the stitch was thought to have absorbed into the wake of the whole mannequin by the influence of the arm.

Figure 16 shows a mannequin CD dressed in various different roughness sportswear, Tights, BA, RA, RB, FA, on a mannequin. In $Re < 2.3 \times 10^5$, there is a difference depending on wears, but in practical competition speed or Reynolds number, all the wears have nearly same value of C_D. In this regard, it is the same result as the effect of C_D of trunk stitches, and it is necessary to consider the influence of the arm.

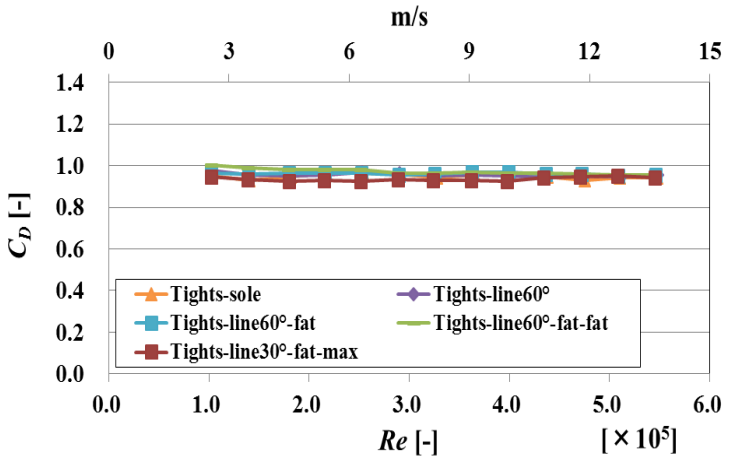

Figure 15. Effect of drag coefficient by the position of seams

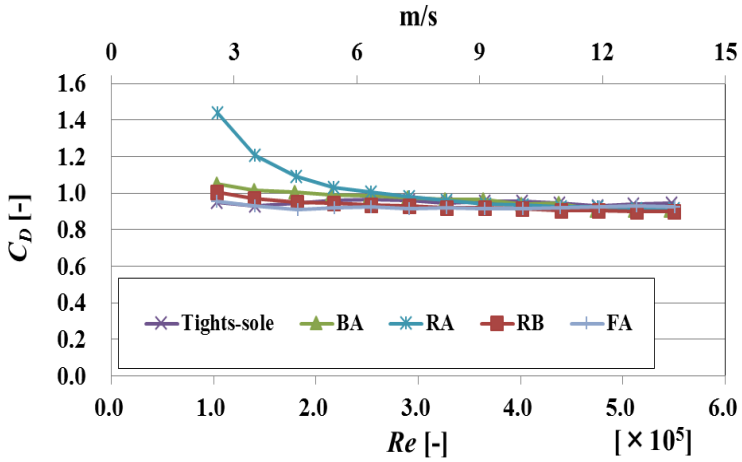

Figure 16. Effect of drag coefficient by different sports wears.

3.4 Experiments on cylinders with arms

3.4.1 Fluid force experiment

Fig.17 shows the result of fluid force measurement with a false stitch placed in the position with the smallest drag of the cylinder. Regarding the drag coefficient C_D, in order to make it easy to compare the magnitude of the drag, the dimensionless processing is performed with the same frontal projected area of only the central representative cylinder. By attaching the arm, the C_D value increased dramatically. Drag crisis induced by stitches occurred in a single cylinder model did not arise either. This is thought to be because the wake flow generated from the stitch as drag crisis was absorbed in the wake flow generated by the arm, so that the decrease of the band width of the wake flow as drag crisis did not occur. Figure 17 also shows the C_D change of cylinders with arms of different arm tilt angles with red circles and blue triangles. However, there was little difference in the C_D value. In the case of tilt angle θ, since separation proceeds by the arm protruding forward as compared with the case of no tilt, it seems that there is no big difference in the wake width as a total.

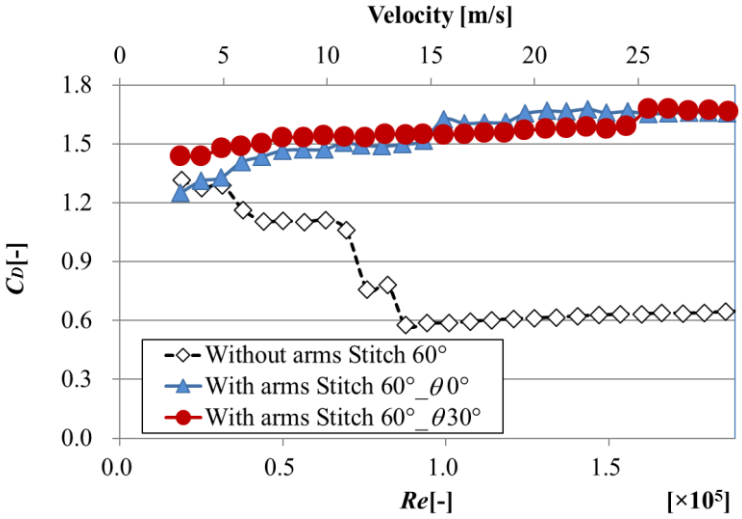

Figure 17. Effect of drag coefficient C_D with/without arms.

3.4.2 PIV measurement

The results of the PIV measurement of the cylinder wake flow are shown in Figures. 18, 19, and 20. Each image represents a flow field of a large area of about 400 mm × 200 mm combining the average flow images of the front and rear of the wake flow. Each shows a velocity vector field of "a single cylinder", "a cylinder with an arm", "a cylinder with an arm tilted by 30°." In each figure, "a" and "b" indicate wind speeds of 10 m/s and 27 m/s, respectively. The color bars in each figure show the range of the wind speed, "a" and "b" are 0 to 10 m/s and 0 to 27 m/s, respectively. In Figures 18, the cylinder has a stitch on the fabric surface. Figure 18a and 18b are the appearance of the flow field before and after the drag crisis. In Figure 18a, the flow separates from the cylindrical surface at 90° ahead, but in Figure 18b, the separation point is displaced backward due to the influence of the stitch. As a result, it is understood that the wake width of Figure 18a is narrower than Figure 18b. This causes drag reduction and drag crisis. However, in Figures 19 and 20 showing the wake velocity field of the cylinder with arms, the width of the wake band is wider than the single cylinder in either case. Moreover, there is a strong ejection flow to the outside from the gap between the arm and the center cylinder as the same speed as the main flow velocity in each velocity condition. It can be said that the witdh is correlated with the result of fluid force measurement. Their C_D curves do not show drag crisis. This is the reason why the turbulent separation from a single cylinder is canceled and the drag crisis does not exist within

this experimental range in the arm cylinder, and also the pressure drag curve is flat in measuring the fluid force of the mannequin. Changing the tilt angle of the cylinder with arms did not affect the C_D value, but also in the PIV measurement, as shown in Figures 19 and 20, no significant difference was found in each downstream flow field as well.

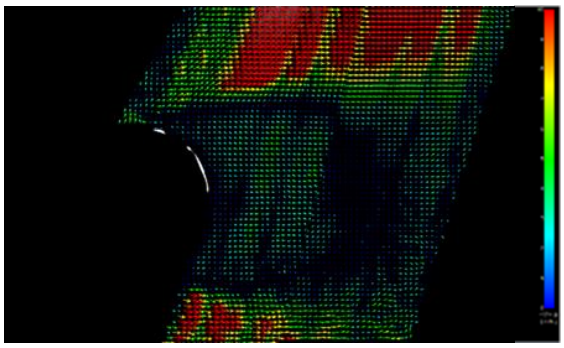

Figure 18a. Wake velocity field of single cylinder at 10 m/s, before drag crisis.

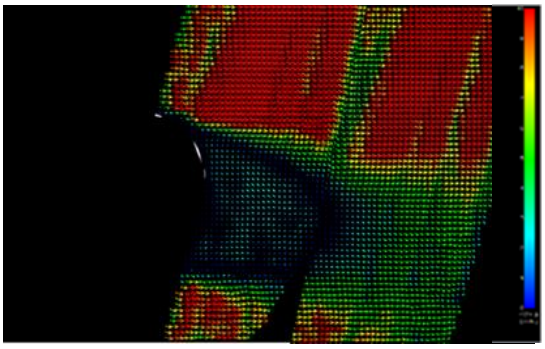

Figure 18b. Wake velocity field of single cylinder at 27 m/s, after drag crisis.

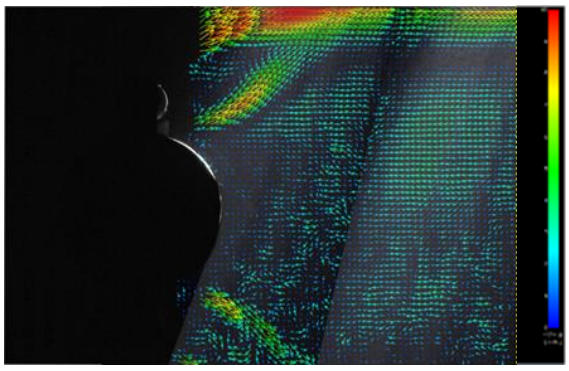

Figure 19a. Wake velocity field of cylinder with arms, no tilt at 10 m/s.

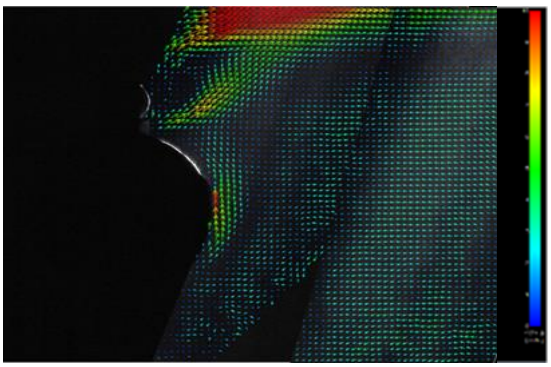

Figure 19b. Wake velocity field of cylinder with arms, no tilt at 27 m/s.

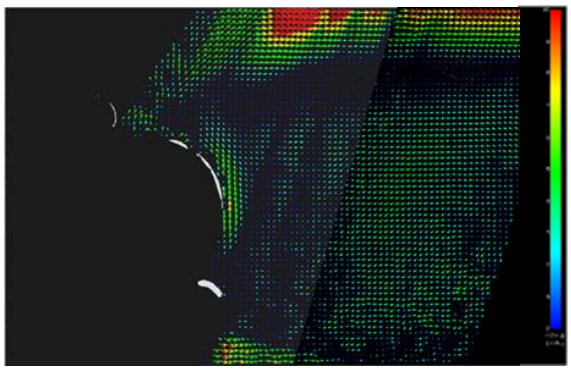

Figure 20a. Wake velocity field of cylinder with arms, tilt angle 30°, at 10 m/s.

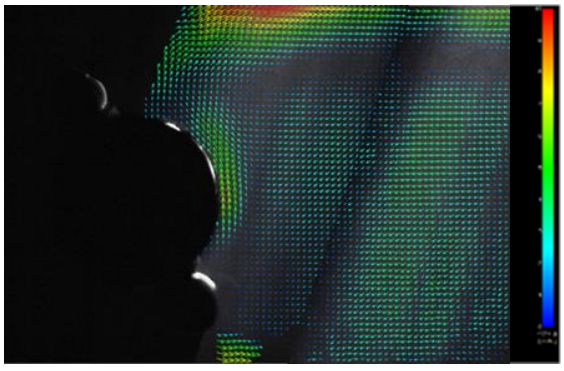

Figure 20b. Wake velocity field of cylinder with arms, tilt angle 30°, at 27 m/s.

3.5 Heat radiation experiment

Figure 21 shows a surface temperature image of a heater with a thermographic camera. In consideration of the flow in the vicinity of the end portion of the cylinder, the average temperature of the square area shown in the center portion in the figure was taken as the measurement temperature of the cylinder. Figures 22a to 22e show the initial temperature and the temperature difference at the end of measurement. for each cloth by setting wind speed. That is, Figures 22 show the heat radiation performance. In each figure, excellent performance indicate as blue hatch, bad one shows as red stripe. At the velocity u = 3 m/s, $Re = 0.2 \times 10^5$, shown in Figures 22a, C_Ds of # 4 and # 5 are about 1 and it is lower than that of other fabrics ($C_D > 1.2$). However in terms of heat radiation performance, # 3 is outstanding and superior. In this Reynolds number region, no drag crisis occurred in the flow field, and the surface should be laminar flow, which indicates that the heat-transfer performance is good due to thin, surface-flattened fabric with high thermal conductivity.

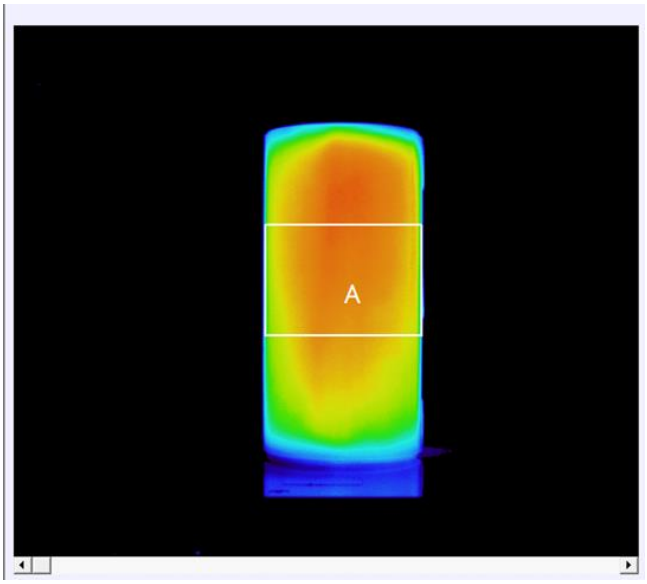

Figure 21. Image of thermo graphy camera and the area of average tempaerature

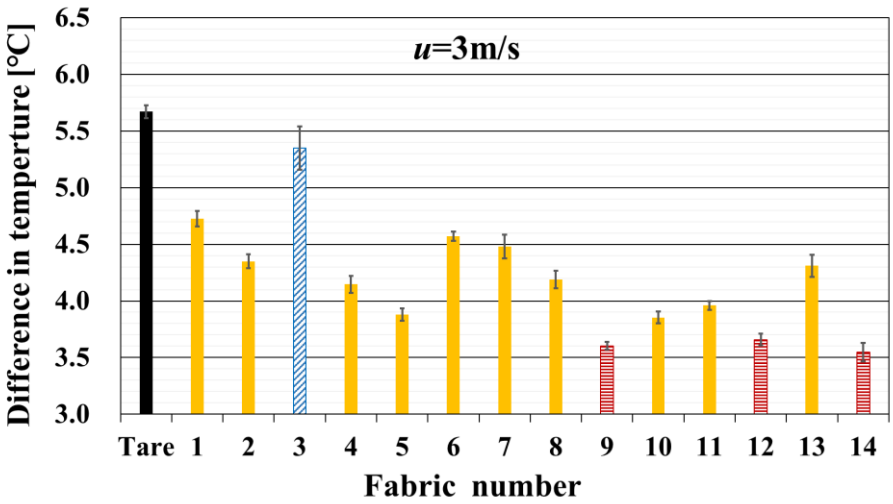

Figure 22a. Heat radiation performance at 3m/s

The heat radiation performance at the velocity u = 6 m/s, Re = 0.4 × 10^5, and u = 9 m/s, Re = 0.6 × 10^5, is shown in Figures 22b and 22c respectively. According to the drag test results, the C_D values of # 4, # 5, # 11, and # 12 are about C_D = 1. Concerning the C_D value of #8, in the recovery mode after drag crisis in these Re, the C_D value=0.9. However, the heat radiation performance was excellent for the fabrics such as # 1, # 3 and # 6. They were thin and the surface was in flat or fine processing. In the laminar flow area, the material with high heat transfer coefficient was found that it is thin and that the surface is in flat processing.

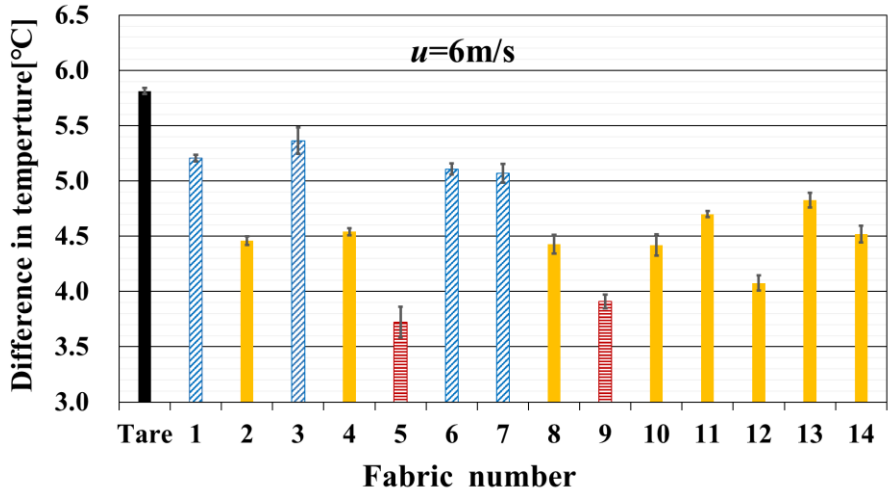

Figure 22b. Heat radiation performance at 6m/s

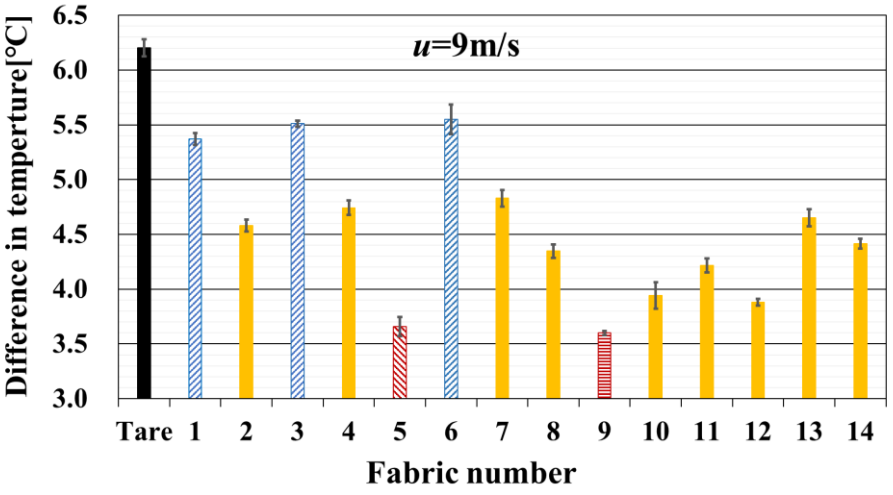

Figure 22c. Heat radiation performance at 9m/s

The results at the velocity u = 12 m/s, Re = 0.8 × 10^5, and u = 15 m/s, Re = 1.0 × 10^5, are shown in Figures 22d and 22e respectively. According to the drag test results, # 9 and # 10 are in drag crisis recovery and their C_D = 0.9. Concerning # 4 and # 5, their flow conditions are during drag crisis and their C_D = 0.7. # 3 and # 12 were also in C_D crisis while C_D = 0.8.

In heat radiation performance, those of # 1, #3 and # 6 are high because their surfaces are on turbulent condition. This seems to be due to turbulent on the fabric surface and this condition increased heat transfer efficiency.

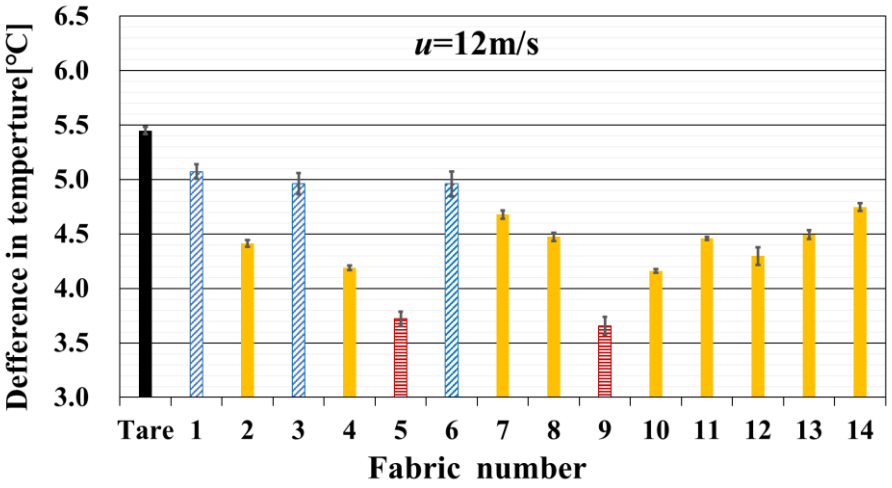

Figure 22d. Heat radiation performance at 12m/s

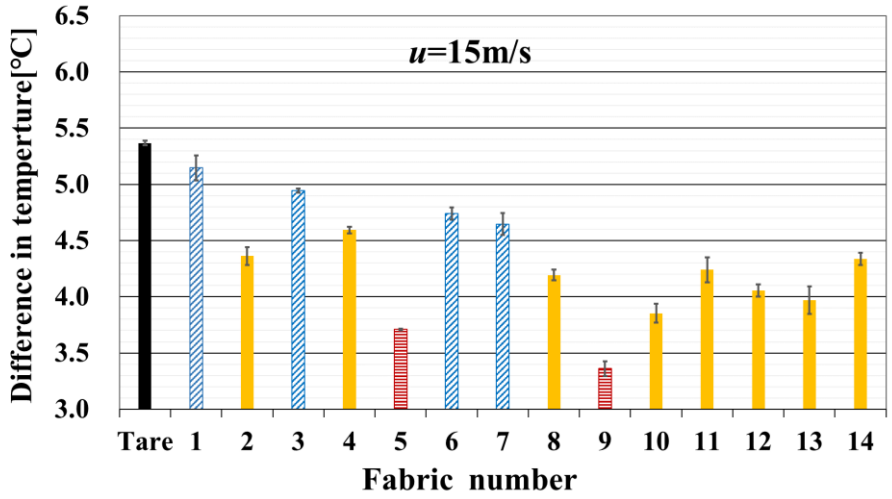

Figure 22e. Heat radiation performance at 15m/s

4. Conclusion

In search of sportswear with low drag and high heat radiation performance, we experimentally investigated changes in fluid drag and heat radiation performance due to various fabrics.

As a result, the following knowledge was obtained:

1. Due to the fabric properties, a sudden decrease in pressure drag, drag crisis, occurs similarly to spheres and cylinders.
2. Drag crisis occurrence range of *Re* varies depending on the roughness of the fabric.
3. In the friction drag measurement, C_f changes due to the difference in surface roughness.
4. It is possible to control the *Re* of occurrence of drag crisis due to the difference in position of the stitch.
5. It is possible to control the *Re* of occurrence of drag crisis due to the difference in stitch shape.
6. As a result of the Mannequin experiment in the standing position, the influence of the stitch is cancelled by the influence of the arm and does not result in the C_D reduction.
   (1) The same phenomenon was confirmed also in a cylinder with arm, and it was confirmed that drag crisis due to turbulent transition did not occur.
   (2) In the visualization of the wake flow by the PIV measurement, correlation was found between the C_D value and the wake flow appearance.
7. In order to mix aerodynamic elements and heat radiation elements, it is important to increase the heat radiation performance by using turbulent flow transitions using thin texture.
8. It is important for improving the heat radiation performance of sportswear that the texture is thin and flat surface processing.

5. References

[1] Gerard H. Kuper, Elmer Sterken, Do skin suits affect the average skating speed?, 2008 *Sports Technology*, Volume 1 Issue 4-5, pp.189-195, John Wiley and Sons Asia Pte Ltd..

[2] S.Luth L. Oggiano, L. M. Bardal and C. Saeter, L. Saetran, Dynamic measurements and drag crisis hysteresis in garment aerodynamics, 2013 *Procedia Engineering* Vol.60, pp.99-105.

[3] Harun Chowdhury, Aerodynamic Design of Sports Garments, 2012 *Applied Aerodynamics*, Dr. Jorge Colman Lerner (Ed.), ISBN: 978-953-51-0611-1, InTech,

[4] Chowdhury, H.; Alam, F.; Mainwaring, D.; Subic, A.; Tate, M.; Forster D. & Beneyto-Ferre, J., Design and Methodology for Evaluating Aerodynamic Characteristics of Sports Textiles, 2009 *Sports Technology*, Vol.2, No.3-4, pp. 81-86, John Wiley and Sons Asia Pte Ltd.

[5] E.Achenbach: Experiments on the flow past spheres at very high Reynolds numbers, 1972 *J. Fluid Mech.* 54, , pp.565-575.

[6] E.Achenbach: The effects of surface roughness and tunnel blockage on the flow past spheres, 1974 *J. Fluid Mech.* 65, pp.113-125.